Dry Adhesion of Polythiophene Nanotube Arrays with Drag-Induced Direction Dependence

Cancan Huang,[1] Kaixuan Sheng,[1] Liangti Qu,[2] Gaoquan Shi[1]

[1]*Department of Chemistry, Tsinghua University, Beijing 100084, People's Republic of China*
[2]*Department of Chemistry, Key Laboratory of Cluster Science, Ministry of Education of China, School of Science, Beijing Institute of Technology, Beijing 100081, People's Republic of China*

Received 11 April 2011; accepted 23 May 2011
DOI 10.1002/app.34941
Published online 29 November 2011 in Wiley Online Library (wileyonlinelibrary.com).

ABSTRACT: Polythiophene (Pth) bilayer films each consists of a nanotube layer and a compact layer had been prepared by electrochemical polymerization and using anodic aluminum oxide (AAO) membranes as template. The films were treated by mechanical polishing and freeze drying to improve the degree of orientation of nanotubes and their surface smoothness. A treated Pth bilayer film can adhere strongly on glass with its nanotube surface by applying a dragging preload. The applied dragging preload caused the original vertically aligned Pth nanotube array to tilt opposite to the direction of preload, which induced a superstrong shear adhesion force of up to 144 ± 30 $N\ cm^{-2}$ for the film with a tube length of 26 μm as the film was dragged along the direction of preload. However, the shear adhesion force opposite to the direction of dragging preload was relatively low (44 ± 17 $N\ cm^{-2}$). The direction-dependent force management of Pth bilayer films is quite similar to that gecko does, indicating the potential for developing advanced adhesive systems.
 J Appl Polym Sci 124: 4047–4053, 2012

Key words: polythiophene; drying adhesion; direction dependence

INTRODUCTION

It is well known that gecko feet have arrays of millions of microscopic hairs (3–130 μm in length), called seta, splitting into hundreds of even smaller nanoscale ends (0.2–0.5 μm in diameter), and called spatula.[1] Gecko can adhere to various surfaces using their physical interactions including van der Waals' and capillary forces between the setae or spatula and the target surfaces.[2–4] Furthermore, the adhered setae can be detached easily by increasing the angles between seta stalks and target surface to be larger than about 30°.[5] It was also found that the shear adhesion force of a gecko seta array tested by dragging the substrate along the natural curvature of seta is much stronger than that against its curvature.[6] This effective management of strong adhesion and easy detachment was considered to be the base of gecko's movement. Inspired by the unique structure and interesting dry adhesive properties of gecko foot, a great deal efforts has been devoted to fabricate artificial dry adhesive tapes.[7] To date, various polymeric nanohair and carbon nanotube (CNTs) films have been investigated for this purpose.[8–22] However, compared with keratin (Young's modulus = 2 GPa), the main component of gecko seta, the mechanical strengths of common polymers (<1 GPa) are usually weak for preparing high-quality adhesive tapes. Although CNTs have extraordinary high mechanical modulus (~ 1000 GPa) and their tapes showed superior adhesion forces,[18–21] the well-aligned structure of CNTs needs to be controlled delicately by high temperature chemical vapor deposition (CVD) process or be pretreated into micropatterns. Therefore, we have developed a readily electrochemical approach to directly synthesize Pth bilayer films for dry adhesive applications.[23] The Pth film has not only high Young's modulus (1.5 GPa), tensile strength (120–130 MPa), and great flexibility,[24,25] but also the length of Pth tubes and the thickness of the supporting film can be well controlled by the integrated charges passed through the electrochemical cell. Actually, the Pth bilayer films have been tested to be able to adhere strongly with their aligned nanotube arrays on smooth glass surface after drying from their wet states under ambient condition.[23] Their normal and shear forces were measured to be 80 ± 8 and 174 ± 10 $N\ cm^{-2}$, respectively. During the drying process, the liquid layer between the nanotube surface and the target surface created an attractive capillary force sufficiently strong to pull the Pth nanotips into contact with the target surface. However, for a dry Pth bilayer film, the nanotubes were easily aggregated into bundles and the tube lengths were polydispersive, which

Correspondence to: G. Shi (gshi@mail.tsinghua.edu.cn).
Contract grant sponsor: Natural Science Foundation of China; contract grant numbers: 91027028, 50873092.

Figure 1 Schematic illustration of the procedures for the post-treatment of the Pth bilayer film. Step 1: mechanical polishing the nanotube surface within AAO template; step 2: removing AAO template and freeze drying. [Color figure can be viewed in the online issue, which is available at wileyonlinelibrary.com.]

largely weakened the adhesion force to target surface and limited their application in dry adhesives.[23,24]

In this article, the Pth bilayer films prepared by the template guided electrodeposition technique reported previously[23,24] were further treated by mechanical polishing and freeze-drying to form highly aligned nanotube arrays with relatively smooth surfaces. The treated films in dried state showed a strong shear adhesion force up to 144 ± 30 N cm^{-2} under a proper dragging preload applied to a Pth bilayer film with a nanotube length of 26 μm. However, opposite to the direction of dragging preload, the shear adhesion force was relatively low at the level of 44 ± 17 N cm^{-2}. The direction-dependent force management of Pth bilayer films is quite similar to that gecko does, indicating the potential for developing advanced adhesive systems.

EXPERIMENTAL

Fabrication of PTh bilayer films

The PTh bilayer films were prepared by electrochemical polymerization of thiophene in boron trifluoride diethyl etherate (BFEE).[23] Electrochemical syntheses were performed in a one-compartment cell using a computer-controlled Model 273 potentiostat-galvanostat (EG and G Princeton Applied Research). The procedures are described briefly as follows. Before the synthesis, the solvent BFEE was purified by distillation, and then stored in the fridge for two days. First, a gold layer with thickness of 20 nm was evaporated onto one side of the AAO membrane with 200 nm pore diameter and 47 mm diameter (Whatman, UK). A stainless steel (SS, AISI 304) electrode with the same area was used as a current collecting electrode and contacted to the gold layer of the membrane. The membrane together with the current collector was fixed between two Teflon rings and used as the working electrode. A circular stainless steel sheet with area of 15.90 cm^2 was used as the counter electrode, and the distance between the working electrode and the counter electrode was about 0.5 cm. All potentials were referred to an Ag/AgCl electrode (immersed directly in the solution). The electrolyte solution is 30 mmol L^{-1} thiophene/BFEE solution, de-aerated by bubbling dry nitrogen before electrochemical polymerization. The structure of the electrolysis cell has been described in Ref. 23. Aligned polythiophene (Pth) nanotubes were grown potentiostatically at 1.3 V (versus Ag/AgCl) and the integrated charge passed during the tubule growth was controlled to be 15–40°C corresponding to the growth of Pth tubes with lengths of 9–36 μm (after mechanical polishing). After the growth of Pth nanotubes, the AAO membrane was overturned to make the gold layer contacted to a platinum wire with diameter around 0.2 mm as the new working electrode for the synthesis of compact Pth film under the same electrochemical conditions. The electrical quantity was controlled to be 20°C. The surface morphology of the samples was studied by using a scanning electron microscope (Hitachi *S*-4500).

Treatment of PTh bilayer films

The PTh nanotube array filled in the AAO template was polished with a sandpaper (1500 meshed) to get a relative smooth surface (Fig. 1). AAO template was removed by using 1 mol L^{-1} NaOH aqueous solution to release the polished Pth bilayer film, followed by washing with deionized water at room temperature to neutral state (PH = 7). Finally, the PTh film was immersed in water and cooled by liquid nitrogen and finally dried under vacuum at −60°C.

Adhesion force measurements

Glass sheets with a root-mean-square (RMS) surface roughness of 1.191 nm (measured by atomic force microscope, SPM 5800, Shimadzu) were used as the target surfaces. The glass surfaces were treated with ethanol, acetone, and deionized water by ultrasonication for 30 min, followed by drying with a nitrogen flow before use. To investigate the adhesive force, a PTh bilayer film was cut into pieces with an area of 0.06–0.12 cm^2. A small piece of PTh film was put on a clean glass with its aligned nanotubes in contact with the glass surface, then the dragging preload was applied by pressing the compact side using a stainless steel plate to give the film a load of 15 N cm^{-2} with movement to one direction at a rate of about 5 mm min^{-1}. The PTh film can adhere strongly to the glass surface after the dragging preload. A thin stainless steel sheet (thickness of 1 mm) with nylon cord was glued on the compact surface

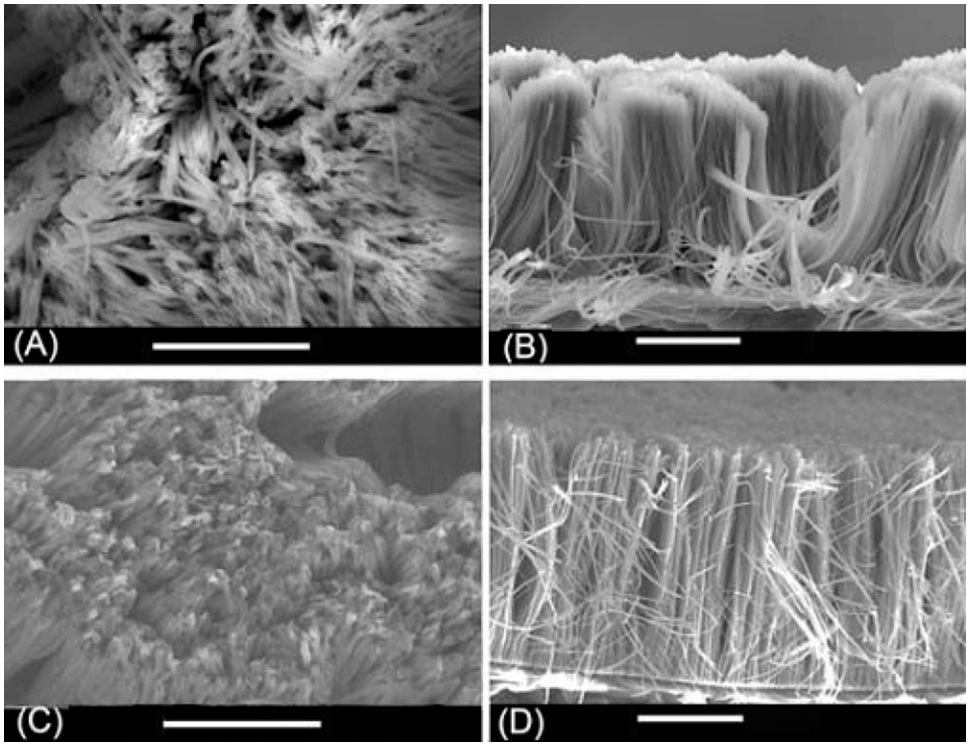

Figure 2 The scanning electron microscope (SEM) images of Pth bilayer films with tube length of 26 μm. (A) Top and (B) side views of an untreated Pth bilayer film; Top (C) and (D) side views of polished wet Pth bilayer film after freeze-drying in vacuum. Scale bar: 5 μm for A, C; 10 μm for B, D.

of the bilayer film as a supporting substrate. One another similar stainless steel sheet (thickness of 1 mm) was also glued on the other end of the glass sheet. The nylon cord is held by the tensile machine (INSTRON 3345) for the adhesion force measurements. The stretching rate was controlled to be 0.05 mm min^{-1}. All measurements were conducted at room temperature and under an environment with humidity around 20%.[26]

RESULTS AND DISCUSSION

The Pth bilayer films were synthesized by electrochemical polymerization of thiophene in boron trifluoride diethyl etherate (BFEE) with aluminum oxide (AAO) as the template according to our previous report.[22,23] However, the Pth nanotubes have a large length polydispersity and they easily aggregate into bundles because of their high specific surface areas and the capillary forces during drying process [Fig. 2(A,B)]. As a result, the Pth bilayer films cannot adhere to target surfaces by finger press. To overcome these problem, we mechanically polished the nanotube surface within the solid AAO template by fine sandpapers (1500 meshes) (See Experimental section), followed with a freeze drying process to avoid the nanotube aggregation. The SEM images of the Pth bilayer films after the treatments of polishing and freeze drying are shown in Figure 2(C,D). Comparing Figure 2(C) with Figure 2(A), the top of Pth array became much more smooth after mechanical polishing. Furthermore, freeze drying treatment also changed most nanotubes bundles formed by normal drying method [Fig. 2(B)] to be well aligned vertically to the compact layer of Pth bilayer film [Fig. 2(D)].

We fabricated a series of Pth bilayer films with tube lengths in the range of 9–36 μm (after mechanical polishing). Therefore, the aspect ratios of the Pth nanotubes were calculated to be 45–180. After polishing and freeze drying treatments, the Pth nanotubes have well-aligned structures and their mouths are open as their lengths are shorter than 26 μm [Fig. 3(A–D)]. The compact layers were controlled to be 2–5 μm in thickness to provide good mechanical strength and flexibility for dry adhesion. It should be noted that the tips of relatively long tubes (e.g., 36 μm) are irregular [Fig. 3(F)] most possibly caused by the nonuniform growth of long tubes.[22,23]

For the measurement of dry adhesion properties, a treated dry PTh bilayer film was put on a clean glass sheet with its aligned tube arrays in contact with glass surface [Fig. 4(A)]. The film showed a weak adhesion force upon applying a vertical preload (<5 $N\ cm^{-2}$). However, it is interesting to find that the film can adhere strongly to glass surface by manually applying a dragging preload along one direction (see Experimental section). Dragging preload

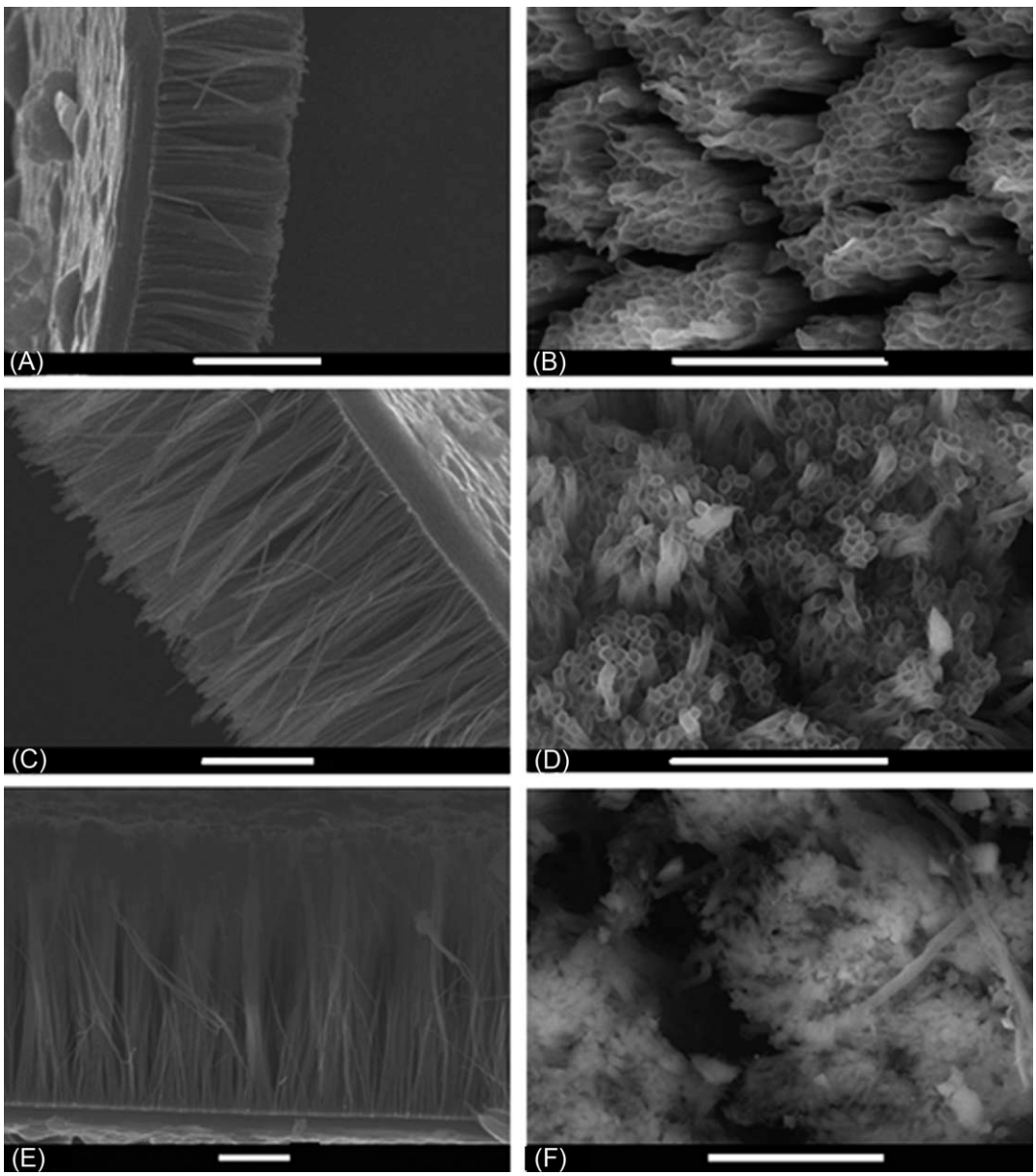

Figure 3 The scanning electron microscope (SEM) images of the Pth bilayer film with tube length of 9 (A, B), 26 (C, D), or 36 μm (E, F). Scale bar: 10 μm for A, C, E; 5 μm for B, D, F.

provided a shear stress to bend the Pth tubes to the opposite direction [Fig. 4(A)]. As a consequence, two distinct shear adhesion forces are produced as shown in Figure 4(A). The one is the shear force measured by dragging the film along the direction of preload (grapping direction), which is defined as F_g, and the other one is against the direction of initial preload (releasing direction), which is defined as F_r. Figure 4(B,C) illustrate the F_g and F_r measured at a slow pull rate of 0.05 mm min^{-1} versus the length of the PTh tubes. As can be seen, F_g increases with the increase of Pth tube length in the range of 9–26 μm. The maximum F_g was measured to be 144 ± 30 N cm^{-2} by using the Pth film with tube length of 26 μm, which is about 14 times that of a gecko foot (10 N cm^{-2}). However, the F_rs of the four films with tube lengths of 9–26 μm were tested to be similar and around 44 ± 17 N cm^{-2}. The Pth bilayer films with short tubule length (e.g., 9 μm) have close F_g and F_r. However, the F_g of the film with long Pth tubes (e.g., 26 μm) is much higher than its F_r. This anisotropic shear forces imply the possible control over the adhesion (conglutination) and release of Pth film on surface.

In analogy to the adhesive mechanism of gecko feet,[2] the adhesion forces of an artificial tape are mainly attributed to the interfacial interactions—van der Waals' forces, usually limited by the contact area. Theoretical studies have indicated that the side contact of fibers to a target surface over a large

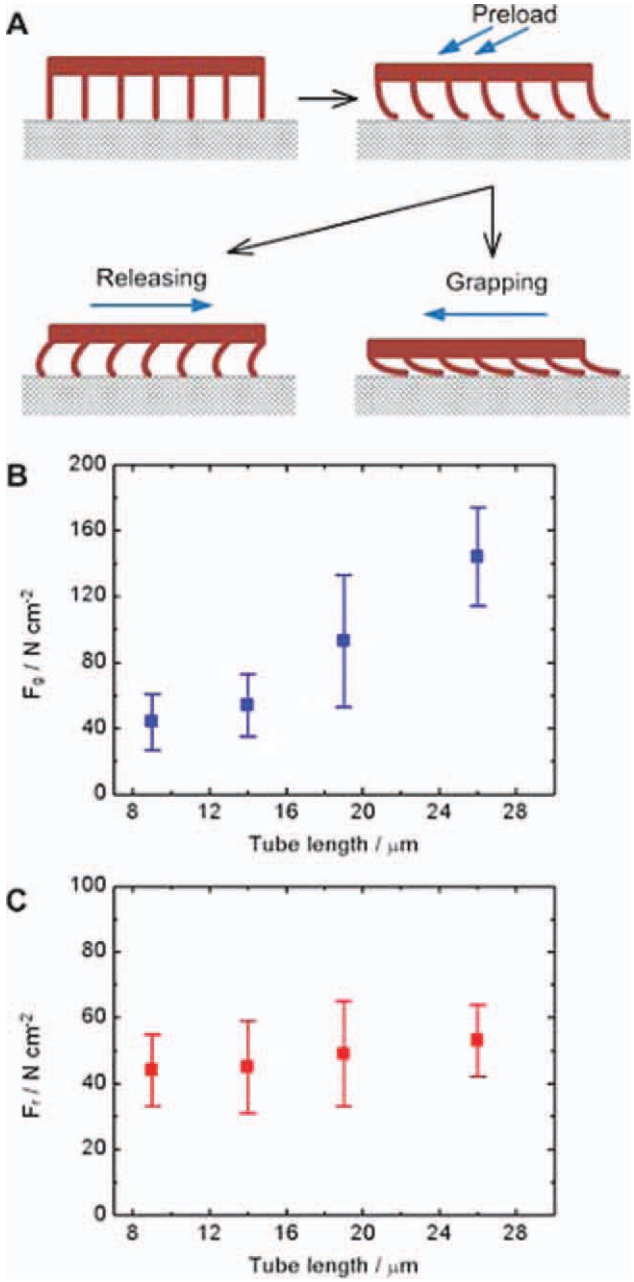

Figure 4 The diagram of preloading and testing the shear forces (A) and the plots of (B) F_g or (C) F_r versus Pth tube length. A shear force was measured for at least 10 repetitions, and analyzed by the standard normal distribution. Film area = 0.06–0.12 cm^2, stretching rate = 0.05 mm min^{-2}. [Color figure can be viewed in the online issue, which is available at wileyonlinelibrary.com.]

contact area could provide a stronger adhesion than that of a tip contact.[27] Therefore, the morphology of the nanotube surface plays a critical role in regulating its adhesive performance. The surface morphologies of the PTh bilayer films with tube lengths <26 μm are similar [Fig. 3(B,D)]. However, the Pth bilayer film with longer tubes has larger aspect ratios and can result in higher elastic energy dissipation within microstructures and more effective contact with target surface, which thus enhances the adhesion force. The electrochemically synthesized Pth has high Young's modulus (1.5 GPa). Thus, it's difficult to bend short tubes (e.g., 9 μm) with low aspect ratio through dragging preload. As a result, the tubes just tilted to some extent and formed tip contacts with target surfaces [Fig. 5(A)]. However, the tubes with lengths as long as 26 μm are sufficiently flexible to bend at their upper parts and form side contacts with target surfaces [Fig. 5(B)].

According to Figure 4, F_g is related to, while F_r is independent on, the tube length of the Pth bilayer film in the scale of 9–26 μm. This could also be attributed to the effective contacts between the nanotube arrays and the target surfaces. When testing the shear force by dragging the film along the direction of preload (F_g), the moving direction of the substrate was in accordance with the curvature of tilting nanotubes (grapping direction), and side contacts could be predominant [Fig. 4(A)]. During the measurement of F_r, however, the substrate moving direction was opposite to the curvature of tilting nanotubes [Fig. 4(A)], and the adhered tubes could be peeled out from the substrate through a "point-by-point" process. These facts are also reflected by the SEM images of the Pth bilayer films after detachment from target surfaces (Fig. 6).

As shown in Figure 6(A) (9-μm tube length) and Figure 6(C) (26-μm tube length), upon dragging in the grapping direction, all the PTh nanotube tips were bent to the same directions. As a result, the Pth tubes adhered and rubbed on the target surfaces to achieve large F_gs. However, as dragged in the releasing direction, the tips of both tube arrays were straightened to some extents to form quasi-dot contacts [Fig. 6(B,D)]. The morphological difference of the surface of 9-μm tube array before and after dragging in both directions is small. Therefore, it exhibited comparable F_g and F_r [Fig. 4(B,C)]. Nevertheless, long nanotubes (e.g., 26 μm) can be lined along the contact surfaces during the F_g test [Fig. 6(C)], which effectively increased the contact area between Pth film and glass surface. Accordingly, the produced shear force is much stronger. However, the surface of long tubes after dragged in the releasing direction showed a disorder morphology [Fig. 6(D), inset], suggesting that the effective contact between Pth film and the glass surface was reduced. As a consequence, the tube tips flipped over the "line" contacts to "dot" contacts for detachment on the target surface in the releasing direction. Thus, in this case, F_r was tested to be much lower than F_g. However, for the PTh film with tube length of 36 μm, the effective contact of tubes with target surface decreased dramatically due to their irregular and defective tube tips [Fig. 3(E,F)]. The available shear force F_g was measured to be only 13 ± 2 N cm^{-2}. The

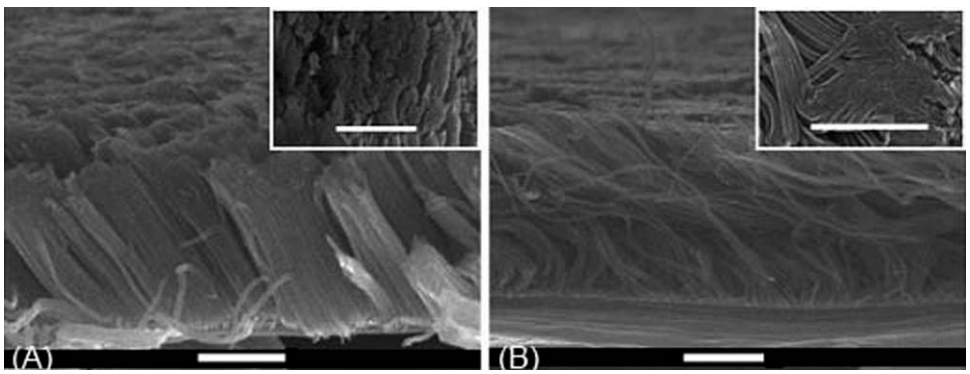

Figure 5 The scanning electron microscope (SEM) images of a PTh bilayer film with tube length of 9 (A) or 26 μm (B) adhered on a glass sheet upon applying a dragging preload and then detached by dragging with a weak normal force. Scale bar: 5 μm.

contribution of the line contact between nanotubes and the substrate to the adhesion force can be estimated by considering the van der Waals interaction. Assume that there is a line contact between nanotubes and the substrate with an effective contact length L (about 1 μm for nanotube length of 26 μm) after preloading. The van der Waals' forces per unit length on the single Pth nanotube is $F_{vdw} = HR^{1/2}/8 \times 2^{1/2}D^{5/2}$[28] where H is the Hamaker constant, The radius of the nanotube $R = 100$ nm, and $D \approx D_0 = 0.165$ nm is the approximate interfacial cut-off distance. H is used 60.5×10^{-21} for polythiopthene, close to that of polyester.[23] The maximum friction force per unit area is $F_g^{max} = \mu F_{vdw} L \rho$[21]; with effective nanotube contact density per unit area ($\rho = 1.91 \times 10^9$ and friction coefficient $\mu = 0.09$, then F_g^{max} is 166 N cm^{-2}. This value is close to the experimental result, 144 ± 30 N cm^{-2}. However, for the PTh bilayer with the short nanotube (e.g., 9 μm), the nanotubes may not have line contact with substrate. Assuming that all of the nanotubes contact with the substrate at their top ends, the van der Waals' forces per unit area is $F_{vdw} = \rho HR/6D^2$, we calculated the maximum force is 71 N cm^{-2}. Compared with the experimental value of 44 ± 17 N cm^{-2}, it can be estimated that at least 61% nanotips interacted with the surface. So the adhesive force could be enhanced by the improving the effective contact area.

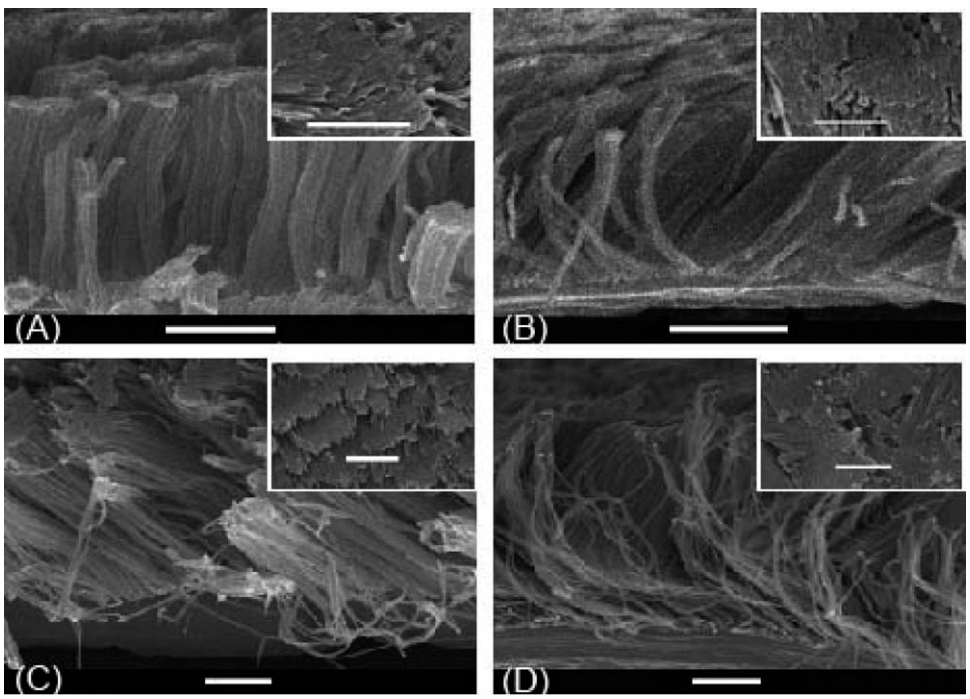

Figure 6 The scanning electron microscope (SEM) images of the Pth bilayer film after detachment in gripping (A and C) and in releasing (B and D) directions. A and B for the PTh bilayer film with tube length of 9 μm; B and D for the PTh bilayer film with tube length of 26 μm. Scale bar: 5 μm.

CONCLUSIONS

Dry adhesives of Pth bilayer films have been treated by mechanically polishing and freeze drying, which are switchable from strong adhesion to easy detachment by controlling over the dragging direction. As demonstrated, the Pth bilayer films consisting of Pth nanotube arrays supported with Pth compact layers can not only adhere strongly on glass surface by dragging preload, but also exhibit direction-dependent adhesion behavior. Superstrong shear adhesion force of up to 144 ± 30 N cm^{-2} has been achieved by dragging the film along the direction of preload for the PTh film with a tube length of 26 μm, which is about 14 times that of a gecko foot. On the contrary, a relatively low adhesion force of 44 ± 17 N cm^{-2} was obtained by dragging the film in the opposite direction, indicating the effective direction-dependent management of the adhesion. In addition, PTh, as one of the typical conducting polymers, which have tunable electrical properties by doping and surface modification, provides a new platform for developing multifunctional adhesive systems.

References

1. Autumn, K.; Liang, Y. A.; Hsieh, S.; Zesch, T. W.; Chan, W. P.; Kenny, T. W.; Fearing, R.; Full, R. J. Nature 2000, 405, 681.
2. Autumn, K.; Peattie, A. M. Integr Comp Biol 2002, 42, 1081.
3. Autumn, K.; Sitti, M.; Liang, Y. A.; Peattie, A. M.; Hansen, W. R.; Sponberg, S. T.; Kenny, W.; Fearing, R.; Israelachvili, J. N.; Full, R. J. Proc Natl Acad Sci USA 2002, 99, 12252.
4. Huber, G.; Mantz, H.; Spolenak, R.; Mecke, K.; Jacobs, K.; Gorb, S. N.; Arzt, E. Proc Natl Acad Sci USA 2005, 102, 16293.
5. Autumn, K.; Dittmore, A.; Santos, D.; Spenko, M.; Cutkosky, M. J Exp Biol 2006, 209, 3569.
6. Autumn, K.; Gravish, N. Philos Trans R Soc A-Math Phys Eng Sci 2008, 366, 1575.
7. Sameoto, D.; Menon, C. Smart Mater Struct 2010, 19, Paper No:103001.
8. Jeong, H. E.; Kwak, R. A.; Khademhosseini, K. Y. Nanoscale 2009, 1, 331.
9. Campo, A. D.; Greiner, C.; Arzt, E. Langmuir 2007, 23, 10235.
10. Trofin, L.; LeDuc, P. R. J Appl Polym Sci 2007, 105, 2549.
11. Boesel, L. F.; Greiner, C.; Arzt, E.; Campo, A. D. Adv Mater 2010, 22, 2125.
12. Geim, A. K.; Dubonos, S. V.; Grigorieva, I. V.; Novoselov, K. S.; Zhukov, A. A.; Shapoval, S. Y. Nat Mater 2003, 2, 461.
13. Jeong, H. E.; Suh, K. Y. Nano Today 2009, 4, 335.
14. Lee, H.; Lee, B. P.; Messersmith, P. B. Nature 2007, 448, 338.
15. Lee, J.; Majidi, C.; Schubert, B.; Fearing, R. S. J R Soc Interface 2008, 5, 835.
16. Schubert, B.; Lee, J.; Majidi, C.; Fearing, R. S. J R Soc Interface 2008, 5, 845.
17. Kim, T. I.; Jeong, H. E.; Suh, K. Y.; Lee, H. H. Adv Mater 2009, 21, 2276.
18. Sethi, S.; Ge, L.; Ci, L.; Aiayan, P. M.; Dhinojwala, A. Nano Lett 2008, 8, 822.
19. Ge, L.; Sethi, S.; Ci, L. P.; Ajayan, M.; Dhinojwala, A. Proc Natl Acad Sci USA 2007, 104, 10792.
20. Qu, L. T.; Dai, L. M. Adv Mater 2007, 19, 3844.
21. Qu, L. T.; Dai, L. M.; Stone, M.; Xia, Z. H.; Wang, Z. L. Science 2008, 322, 238.
22. Ho, A. Y. Y.; Yeo, L. P.; Lam, Y. C.; Rodriguez, I. ACS Nano 2011, 5, 10.1021/nn103191q.
23. Lu, G. W.; Hong, W. J.; Tong, L.; Bai, H.; Wei, Y.; Shi, G. Q. ACS Nano 2008, 2, 2342.
24. Shi, G. Q.; Jin, S.; Xue, G.; Li, C. Science 1995, 267, 994.
25. Fu, M. X. Y.; Zhu, F. R.; Tan, Q.; Shi, G. Q. Adv Mater 2001, 13, 1874.
26. Wang, X. L.; Bai, H.; Shi, G. Q. J Am Chem Soc 2011, 133, 6338.
27. Majidi, C. S.; Groff, R. E.; Fearing, R. S. J Appl Phys 2005, 98, Paper No:103521.
28. Leckband, D.; Israelachvili, J. Quarterly Rev Biophys 2001, 34, 105.